Using 3D seismic data to study damage zones

Abstract

Damage zones can observationally link earthquake physics to mechanics beyond elasticity. The extent of distributed damage affects an earthquake's propagation, its associated strong motion and perhaps even the distribution of seismicity around the fault. However, 3D observations of damage remain limited. Here we constrain damage zones offshore California using existing 3D seismic reflection datasets. Our current results from the Palo Verdes Fault zone show that damage is most concentrated around mapped faults and decays exponentially to a distance of 2.2 km, where fracturing with distance from the mapped fault and reaches a clearly defined and relatively undamaged background values for all examined depths and lithologies (450 m to 2.2 km). We also find that the damage decay and background level damage in the background differs for each unit indicating that lithology is a major control on damage variability, but not depth. Qualitatively less brittle units, such as siltstone, appear to have damage that decays slowly, but also have low background damage levels and the opposite is true for sandstone and conglomerate. Surprisingly, these differences in damage decay and background level balance each other out to result in a consistent damage zone width regardless of lithology or depth. We will follow up on these observations by exploring potential damage asymmetry and the relationship to folding. This work is being performed by UC Santa Cruz graduate student Travis Alongi in collaboration with Danny Brothers and Jared Kluesner of the USGS.

Introduction and Preliminary Work

Faults at field and laboratory scales are observed to be complex damage zones in response to repeated rupture propagation. This damage zone plays a role in rupture, attenuation and perhaps even nucleation. However, basic knowledge of its systematics is limited and thus models of its effects are handicapped. Previous studies have investigated damage zone systematics based on exposed fracture density and related observations (Keren & Kirkpatrick, 2016; Mitchell & Faulkner, 2009; Savage & Brodsky, 2011; Scholz et al., 1993; Shipton et al., 2006; Wilson et al., 2003). However, these studies have been largely limited to surficial measurements of fracture density and lacked the means to quantify the damage in situ at seismogenic depths. In particular, it is difficult to address questions of depth, lithology and stress regime dependence through the geological measurements available.

Seismic data has contributed significantly to our understanding of fault damage zones (Ben-Zion et al., 2003; Cochran et al., 2009; Vidale & Li, 2003). However, experiments and techniques are limited by access and deployment logistics on land. Active source marine seismic data may provide a means to improve the situation. Seismic reflection data has the capability of observing faults and fractures *in situ* using advanced object detection approaches and these techniques are burgeoning with the machine-learning revolution (Edwards et al., 2018; Kluesner & Brothers, 2016), but the prohibitively high acquisition and processing cost of the 3D volumes have limited the use for academic purposes and fault mechanics applications. Proprietary holds on industry collected 3D

marine seismic reflection data have recently expired, and these datasets are becoming available through the USGS.

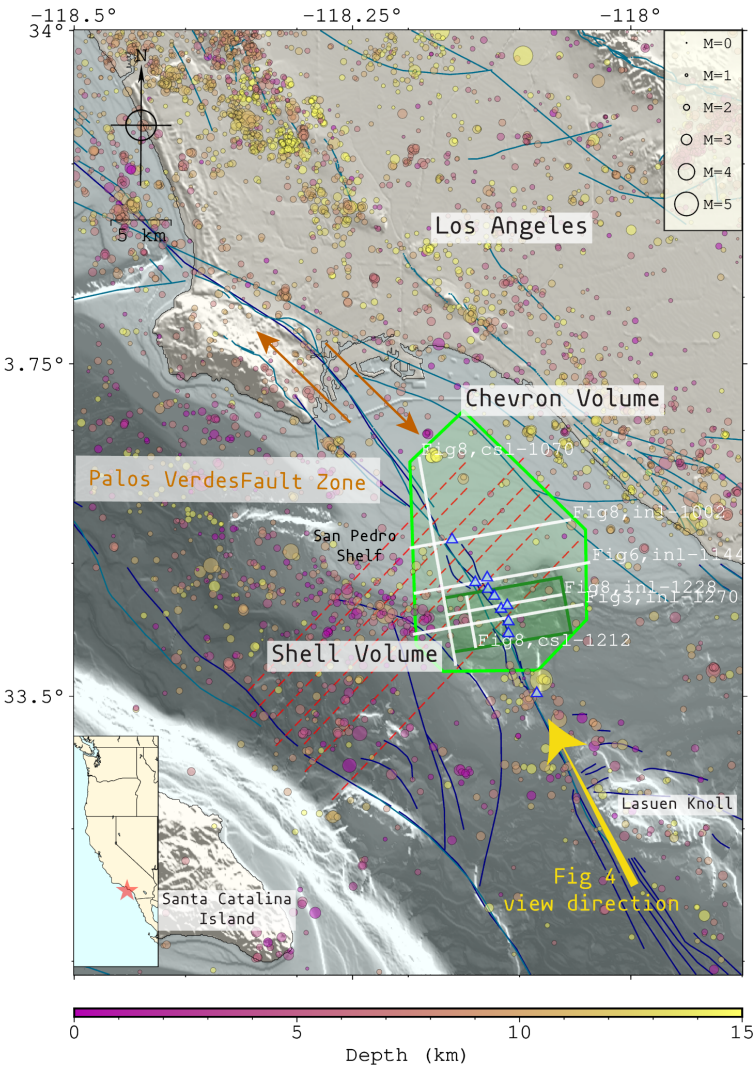

Figure 1. Map of southern California Inner Borderlands and San Pedro Shelf. Inset map shows western US with the red star indicating the study area. Main map shows location of mapped fault traces from the USGS quaternary faults database, where the navy-blue lines are the USGS offshore Quaternary faults (Walton et al., 2020) dataset and the turquoise lines are the USGS onshore Quaternary faults (U.S. Geological Survey and California Geologic Survey, Quaternary fault and fold database for the United States, accessed August 2019). Thick green polygons indicate the bounds of the 3D marine active source data sets. Dashed red lines indicate the 2D lines used in the study. The blue triangles indicate the surface location of the geophysical well logs. White lines are the location of cross-sections of lines shown in other figures. Yellow arrow is the view direction from figure 4. Circles indicate earthquakes colored by depth and scaled by magnitude from the Southern California Earthquake Data Center alternate catalog [1981 - 2018] (Hauksson et al., 2012).

Prior SCEC-funded Work

This work is a continuation of a SCEC-funded project. Through our SCEC-funded project, we utilized 3D marine seismic surveys collected offshore Los Angeles over the San Pedro shelf and slope, spanning ~20 km of the Palo Verdes fault to measure fault zone damage (Figure 1). We used a Thin Fault Likelihood algorithm to measure seismically imaged fractures (Hale, 2012) and demonstrate that the fracture zones identified by this method are preferentially near fault strands, as expected for damage zones. This analysis reveals depth dependent fault zone damage and allows for an evaluation of damage formation as a function of depth and lithology.

In the last year, we have separated the data by geological unit (Figure 2). There is a clear relationship of exponential damage decay with distance from the Palos Verdes Fault. These relationship observations are similar to what is seen in outcrop scale

studies. We infer a ~2 km half-width of the damage zone regardless of lithology (Figure 2).

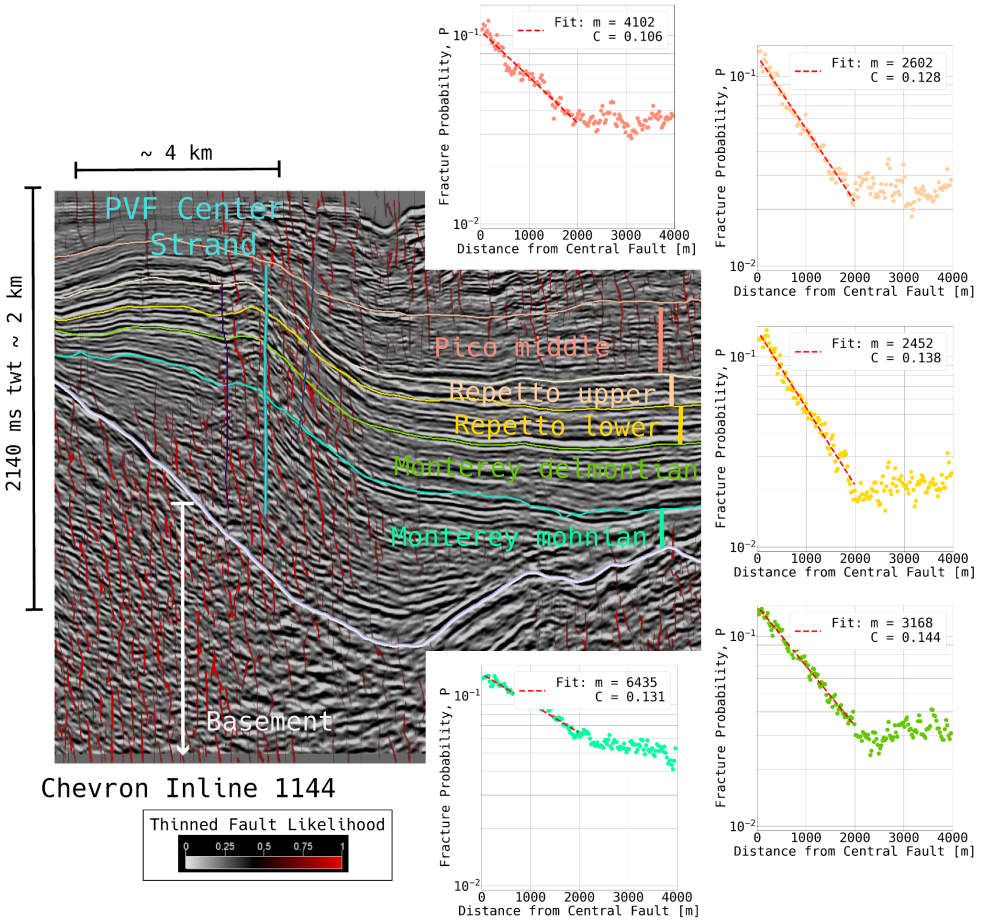

Figure 2. The left figure shows an example of dip-steered diffusion filtered seismic data in black and white color scale(location shown in Figure 1). Overlain, the vertical teal line is the manually mapped central strand, the dark purple is the western strand, and the navy blue is the eastern strand. The transparent to red is the Thinned Fault Likelihood fault detections. The multi-color horizontal lines are mapped 3D horizon-surfaces projected onto the inline and mark lithological contacts or unconformities that have been tied to well logs. These horizons are used as upper and lower bounds to constrain the fracture probability as a function of distance for each lithology within the Chevron volume, which are shown in the semi-log plots on the right of the figure. Note the different exponential fit slopes in different geologic units and variable background (horizontal portion).

The new window into damage as a function of lithology and depth provides a new insight into the trade-off between background damage and decay. Qualitatively stronger units decay quickly with distance, but have low background levels. The opposite is true for softer units such as siltstone. Interestingly, these factors counterbalance each other resulting in a consistent damage width across the units. The data indicates that width can be a more stable feature of damage zones than might be anticipated from observed variations in individual units. This new observation invites future modelling work

exploring the role of rock strength in controlling damage zone width. Apparently the relationship involves non-trivial feedback mechanisms that needs to be fully explored.

The SCEC funding has supported graduate student Travis Alongi and engaged the USGS Coastal Hazards group in the SCEC collaboration. This year Alongi made substantial progress once COVID-related delays were resolved. In the course of the analysis, we realized that separating the data by geological units was a key step that had not been in our original work plan. This separation led to the key insights about the importance of geology in controlling both decay and background in complementary ways as discussed above. Alongi also expanded analysis to the higher resolution Shell volume this year.

References

Alongi, T., Brodsky, E. E., Kluesner, J. W., & Brothers, D. S. (2019). Fault Damage Zones in 3D with Active-Source Seismic Data. Presented at the Southern California Earthquake Center Annual Meeting, Palm Springs, CA.

Ben-Zion, Y., Peng, Z., Okaya, D., Seeber, L., Armbruster, J. G., Ozer, N., et al. (2003). A shallow fault-zone structure illuminated by trapped waves in the Karadere–Duzce branch of the North Anatolian Fault, western Turkey. *Geophysical Journal International*, *152*(3), 699–717. https://doi.org/10.1046/j.1365-246X.2003.01870.x

Brodsky, E. E., & Lajoie, L. J. (2013). Anthropogenic seismicity rates and operational parameters at the Salton Sea Geothermal Field. *Science*, *341*(6), 543–546.

Cochran, E. S., Li, Y.-G., Shearer, P. M., Barbot, S., Fialko, Y., & Vidale, J. E. (2009). Seismic and geodetic evidence for extensive, long-lived fault damage zones. *Geology*, *37*(4), 315–318. https://doi.org/10.1130/G25306A.1

Dor, O., Rockwell, T. K., & Ben-Zion, Y. (2006). Geological observations of damage asymmetry in the structure of the San Jacinto, San Andreas and Punchbowl faults in Southern California: A possible indicator for preferred rupture propagation direction. *Pure and Applied Geophysics*, *163*(2), 301-349.

Edwards, J. H., Kluesner, J. W., Silver, E. A., Brodsky, E. E., Brothers, D. S., Bangs, N. L., et al. (2018). Corrugated megathrust revealed offshore from Costa Rica. *Nature Geoscience*, *11*(3), 197–202. https://doi.org/10.1038/s41561-018-0061-4

Hale, D. (2012). Fault surfaces and fault throws from 3D seismic images. In *SEG Technical Program Expanded Abstracts 2012* (pp. 1–6). Society of Exploration Geophysicists. https://doi.org/10.1190/segam2012-0734.1

Hauksson, E., Yang, W., & Shearer, P. M. (2012). Waveform Relocated Earthquake Catalog for Southern California (1981 to June 2011). *Bulletin Of The Seismological Society Of America*, *102*(5), 2239–2244. https://doi.org/10.1785/0120120010

Keren, T. T., & Kirkpatrick, J. D. (2016). The damage is done: Low fault friction recorded in the damage zone of the shallow Japan Trench décollement. *Journal of Geophysical Research: Solid Earth*, *121*(5), 3804–3824. https://doi.org/10.1002/2015JB012311

Kluesner, J. W., & Brothers, D. S. (2016). Seismic attribute detection of faults and fluid pathways within an active strike-slip shear zone: New insights from high-resolution 3D P-Cable™ seismic data along the Hosgri Fault, offshore California. *Interpretation*, *4*(1), SB131–SB148. https://doi.org/10.1190/INT-2015-0143.1

Lockner, D. A., Morrow, C., Moore, D., & Hickman, S. (2011). Low strength of deep San Andreas fault gouge from SAFOD core. *Nature*, *472*(7341), 82–85. https://doi.org/10.1038/nature09927

Mitchell, T. M., & Faulkner, D. R. (2009). The nature and origin of off-fault damage surrounding strike-slip fault zones with a wide range of displacements: A field study from the Atacama fault system, northern Chile. *Journal of Structural Geology*, *31*(8), 802–816. https://doi.org/10.1016/j.jsg.2009.05.002

Sagy, A., Brodsky, E. E., & Axen, G. (2007). Evolution of fault-surface roughness with slip. *Geology*, *35*(3), 283–286.

Savage, H. M., & Brodsky, E. E. (2011). Collateral damage: Evolution with displacement of fracture distribution and secondary fault strands in fault damage zones. *Journal of Geophysical Research*, *116*(B), 03405. https://doi.org/10.1029/2010JB007665

Scholz, C., Dawers, N., Yu, J., Anders, M., & Cowie, P. (1993). Fault growth and fault scaling laws: preliminary results. *Journal of Geophysical Research*, *98*(B12), 21951.

Scholz, C. H. (2002). *The Mechanics of Earthquakes and Faulting*. Cambridge, UK: Cambridge University Press.

Shipton, Z., Evans, J., Abercrombie, R., & Brodsky, E. E. (2006). The missing sinks: slip localization in faults, damage zones, and the seismic energy budget.

Sylvester, A. (1988). Strike-Slip faults. *GSA Bulletin*, *100*, 1666–1703. https://doi.org/10.1130/0016-7606(1988)100<1666:SSF>2.3.CO;2

Vidale, J. E., & Li, Y.-G. (2003). Damage to the shallow Landers fault from the nearby Hector Mine earthquake. *Nature*, *421*(6922), 524–526. https://doi.org/10.1038/nature01354

Wilson, J. E., Chester, J. S., & Chester, F. M. (2003). Microfracture analysis of fault growth and wear processes, Punchbowl Fault, San Andreas system, California. *Journal*

of Structural Geology, *25*(11), 1855–1873. https://doi.org/10.1016/S0191-8141(03)00036-1